Artifact Due to B_0 Fluctuations in fMRI: Correction Using the *k*-Space Central Line

Emmanuel Durand,[1,2]* Pierre-François van de Moortele,[2] Mathilde Pachot-Clouard,[2] and Denis Le Bihan[2]

Magnetic resonance experiments require the main magnetic field, B_0, to remain very stable. Several external sources, such as moving ferromagnetic objects and/or changing electromagnetic fields, can significantly change the value of B_0 over time. This work describes an apparent displacement along the phase-encoding axis caused by a variation in B_0. This artifact was observed in fMRI images acquired with EPI. The effect was characterized and tested using an immobile phantom. The image displacement motion along the phase-encoding axis closely followed the changes in B_0. The phase of the central line in the Fourier space was successfully used to correct this artifact. Fluctuations in B_0 may result in artifacts that mimic subject head motion, and must be appropriately corrected. Magn Reson Med 46:198–201, 2001. © 2001 Wiley-Liss, Inc.

Key words: fMRI; B_0 stability; artifacts; EPI; navigator echo

The stability of the principal magnetic field, B_0, is critical for MRI experiments. This is especially true for EPI based images, which are very sensitive to phase shifts occurring during long echo train acquisitions, as there is no self-rephasing of the echoes. If the instability occurs with a time scale shorter than the time required to acquire an image, the resulting phase-shift will produce ghost artifacts in the phase-encoding direction (1–3). If it occurs with a longer time scale, the phase-shift will produce image-to-image changes that may be misinterpreted in fMRI experiments as subject head motion or false cortical activation (4). Although most MRI systems are designed to minimize the effect of external sources of magnetic perturbations, moving ferromagnetic objects, such as cars, or changes in electromagnetic fields caused by power lines may have residual effects. The intensity of the effect depends on many parameters, such as the distance between the magnetic or electrical source and the magnet, the design of the magnet and its shielding, and the type of MRI sequence (3,4). This report describes the effect of fluctuations in B_0 produced on a 1.5 T whole-body MRI scanner by a nearby train power line. The artifacts observed in fMRI experiments were characterized using a phantom and corrected with a self-navigator echo (5) algorithm using the *k*-space center line.

THEORY

We refer to the readout, phase-encoding, and slice-selection axes as *x*, *y*, and *z*. Let us consider $\Delta B_0(t)$, the time-dependent variation in the principal magnetic field around its nominal value B_0 (we do not consider the fields produced by the gradient coils). We shall assume that $\Delta B_0(t)$ is slow enough to be considered as constant during the acquisition of one image. The effect of ΔB_0 will therefore be a constant and additional phase shift of the signal occurring during the interval between the radiofrequency (RF) pulse to the signal readout:

$$\varphi(t) = \gamma \Delta B_0 t \quad [1]$$

where γ is the gyro-magnetic ratio. If τ_y is the time between the beginning of the acquisition of two consecutive lines in the *k*-space, ΔB_0 will result in a phase shift $\delta\phi$ between these lines with:

$$\delta\varphi = \gamma \Delta B_0 \tau_y. \quad [2]$$

This phase shift is the same as that produced by a displacement δy along the *y*-axis provided that:

$$k_y \delta y = \gamma \Delta B_0 \tau_y \quad [3]$$

where $k_y = \gamma \int G_y(t)dt$. Though a phase shift also occurs along the readout axis, it is negligible in practice.

Before such an artifact can be corrected we must know the value of ΔB_0 for each acquisition, and then compensate for the phase shifts between the lines. A parameter that varies during signal acquisition can be measured with a navigator echo (4,6). If the navigator echo is acquired at a time T after the RF pulse, the effect of ΔB_0 will be to shift the average phase of the navigator echo $\Delta\Phi$ of $\gamma T \Delta B_0$ (7). Hence, the change ΔB_0 is identified by:

$$\Delta B_0 = \frac{\Delta\Phi}{\gamma T}. \quad [4]$$

MATERIALS AND METHODS

We noticed large displacements of images in the phase-encoding direction during preliminary fMRI experiments conducted at our institution. These could not be explained by subject motion. As our site lies close to an electrical train line (DC current), we postulated that variations in B_0 were caused by the current in the catenaries. Experiments were carried out on a static phantom made of a 20-cm plastic sphere filled with doped water to characterize and correct the artifact.

[1]Unité de Recherche en Résonance Magnétique Médicale, Le Kremlin-Bicêtre, France.

[2]Service Hospitalier Frédéric Joliot, Direction des Sciences du Vivant, Commissariat à l'Énergie Atomique, Orsay, France.

*Correspondence to: E. Durand, Unité de Recherche en Résonance Magnétique Médicale (U2R2M), CHU Bicêtre, 78 rue du Général Leclerc, F 94275 Le Kremlin-Bicêtre Cedex, France. E-mail: emmanuel.durand@cierm.u-psud.fr

Received 31 March 2000; revised 16 January 2001; accepted 17 January 2001.

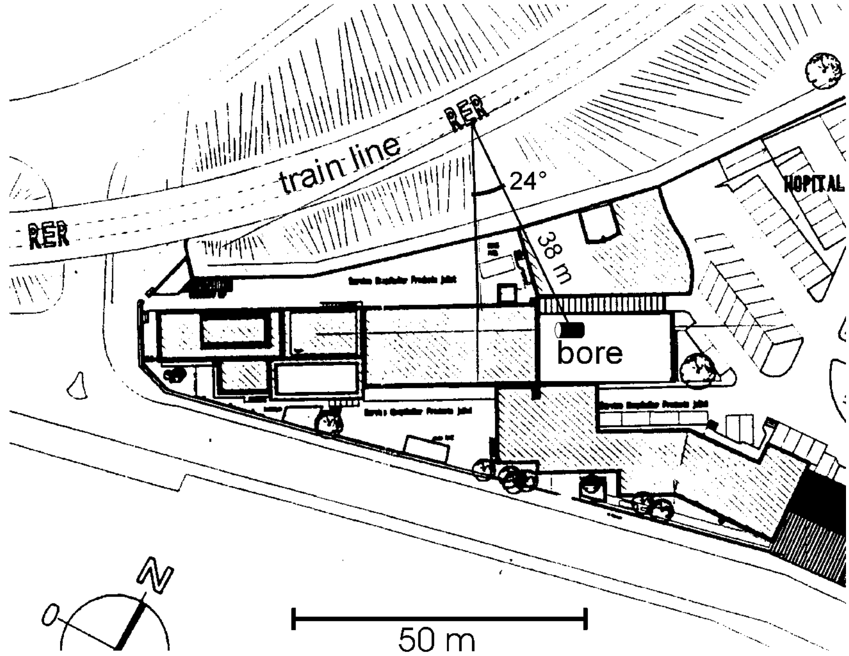

FIG. 1. Site map indicating the locations of the train track and the magnet bore.

All the images were acquired on a standard 1.5 T GE Signa Horizon unit (General Electric, Milwaukee, WI) equipped with an actively shielded superconducting magnet and high-power gradient coils (23 mT.m^{-1}). The magnet was installed in a room without magnetic shielding. The shortest distance between the center of the magnet and the train track was 38 m. The angle between the direction of B_0 and that of the track was 24° (Fig. 1).

The sequence used was a blipped single-shot gradient-echo EPI, with a 20° flip angle. The echo time (TE) was 60 ms, the reception bandwidth was 125 kHz, and the field of view was 22 × 22 cm^2 with a 64 × 64 matrix. The signal was not sampled during the ramps. Thirty-six 3.5-mm-thick contiguous slices were acquired 53 times at intervals (TR) of 6 s. The time between the beginning of two consecutive lines was τ_y = 719 μs. One reference scan was acquired without phase encoding before each series of images (8). We used the central line of the Fourier space as a self-navigator echo (5) instead of a classical navigator echo (6), distinct from the main echo train.

The imaging sequence differed from that provided by the manufacturer in two ways. First, the software was modified to acquire 53 series of 36 contiguous slices (1908 images), as the manufacturer's database did not permit the acquisition of more than 512 images at the same time. We also modified the original sequence, which was designed to acquire symmetrically 32 lines on each side of the central line of the Fourier space, without the central line, to acquire the central line along with 32 positive and 31 negative lines. The signal corresponding to this central line is hereafter referred to as the self-navigator. As usual, a reference image was acquired with the same parameters before each acquisition, but with only two repetitions and no phase-encoding gradients to correct the time shift between odd and even echoes. These imaging parameters were typical of those used routinely in our institution for BOLD fMRI experiments conducted on human subjects.

All images were reconstructed as usual by reversing every second line, applying a Hamming filter in both directions, 1D Fourier transforming along the readout axis, and correcting the phase in the hybrid space to remove the Nyquist ghost (8). The average phase of the central line of each slice was then calculated in the hybrid space to determine ΔB_0 (9), each point being weighted by its squared magnitude. A zero-order phase shift comes down to multiplying the data by the constant $e^{-i \cdot \Delta\Phi}$. Hence, as the Fourier transform is linear, this zero-order phase shift may be determined in the *k*-space as well as in the hybrid space. The phase time-course along sequentially acquired images was unwrapped to avoid phase jumps between $+\pi$ and $-\pi$ using a simple algorithm: if the phase difference between two successive images exceeded π, then 2π was added (or subtracted) to the latest phase value. Then, $\Delta\Phi(t)$, the difference between the average phase of the image acquired at time t and the average phase of the image acquired at time 0 was used to determine $\Delta B_0(t)$, the change in the magnetic field between times 0 and t, according to:

$$\Delta B_0(t) = \Delta\Phi(t)/(\gamma TE). \quad [5]$$

The signal was corrected for the B_0 drift by multiplying each line signal, $S(x,j)$, by a first-order phase-shift factor:

$$S'(x, j) = S(x, j)\exp(-i\gamma\Delta B_0(t)\tau_y j) \quad [6]$$

where j is the line number and τ_y the time between the beginning of two consecutive lines. We assumed that the phase shift due to the B_0 drift was negligible within one line. Finally, the data were Fourier transformed in the phase-encoding direction to get the corrected image.

A "center-of-mass" was calculated for each image using custom C-software to quantify the displacement of the object in the image. This "center-of-mass" was obtained by averaging the coordinates of each pixel weighted by the corresponding signal magnitude, and was plotted against time before and after correcting for the fluctuation in B_0.

RESULTS

Figure 2a shows the variation of the phantom center-of-mass before correction along the three space directions plotted against time. Whereas the apparent motion was negligible along the readout and slice-selection axes, it appeared to be much larger (over 0.5 mm) along the phase-encoding axis. It also exhibited large, slow fluctuations with a pseudoperiod of about 2 min. Figure 3 shows the calculated values for $\Delta B_0(t)$ plotted against time for three slice levels. The amplitude of this variation was about 1.10^{-7} T (0.08 ppm or 5 Hz). The time-course of $\Delta B_0(t)$ and the center-of-mass along the phase-encoding directions looked very similar.

Figure 2b shows the variation in the phantom center-of-mass after corrections. The apparent motion along the *y*-axis was greatly reduced to become comparable to that along the *x*-axis. The apparent motion along *z* remained somewhat greater (about 0.2 mm) than in the other directions, and showed a trend towards negative values. Data processing did not impair image quality, which was similar before and after the B_0 drift correction.

The experiments were repeated in the middle of the night when no trains were running. These experiments showed that the displacement was reduced to noise level (under 0.1 mm) in the phantom image.

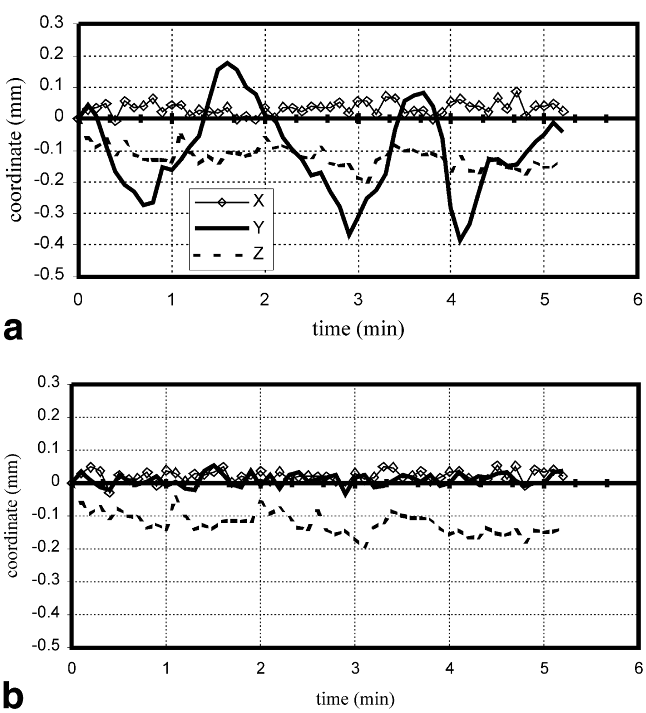

FIG. 2. Coordinates of the phantom "center of mass" plotted against time (**a**) before and (**b**) after correction. *x*, *y*, and *z* are the readout, phase-encoding, and slice-selection axes, respectively.

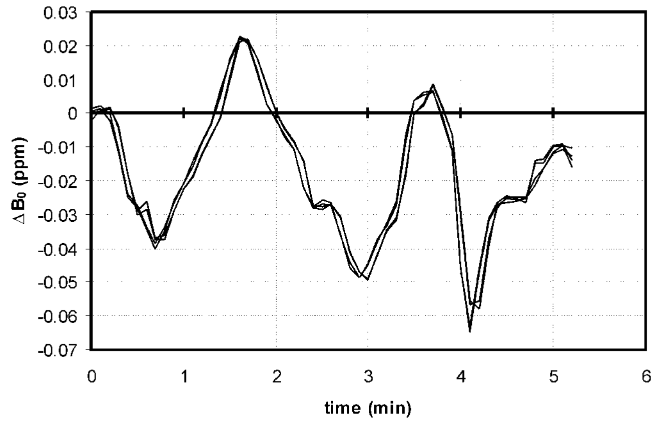

FIG. 3. Principal fluctuations in the magnetic field plotted against time for three slice levels.

Once fluctuations in B_0 had been identified as the source of artifact at our site, the MRI system was magnetically shielded with mu-metal. This shielding was only partially successful: it reduced the fluctuations by 50%. A correction device using a feedback sensor was then installed, which lowered the fluctuations to within the manufacturer's specifications (2 Hz).

DISCUSSION

The patterns of plots of the *y*-coordinate of the center-of-mass and the B_0 fluctuations against time (Fig. 2a and b) were very similar, although there is no intrinsic correlation between the calculation of the two (the B_0 fluctuations were calculated on the central line, which is not phase encoded). This strongly supports our initial postulation that the fluctuations in B_0 were responsible for the apparent motion seen along the *y*-axis using a static phantom. These plots showed a rather slow variation compared to the sampling time of B_0 (6 s), supporting the assumption that there was no significant variation of B_0 during the interval between the RF pulse and data sampling.

The apparent motion width along the phase-encoding axis was significantly reduced after correction. It was of the same order of magnitude as the residual apparent motion along the readout axis, and the initial pseudoperiodic pattern was no longer seen. The residual slight apparent motion along the slice-selection axis could be due to long-term eddy currents, or to a true displacement of the phantom in the bore rails because of gradient vibrations. The method described here is designed to detect and correct the pseudomotion artifact that occurs along the phase-encoding axis by using the average phase of the central line to detrend B_0 fluctuations. However, it will not correct true motion along this axis, since the central line is not phase encoded.

The train company informed us that the current intensity in their lines was about 10000 A, with variations of up to several thousand amps over a time scale of minutes. These variations are generated by the acceleration and active braking of the trains. We calculated the theoretical magnetic field induced in the magnet room by the power line, using a simple model of two infinite current straight lines, one for the catenary and one for the return current assumed to be in the rail tracks (cf., Fig. 1). If h is the height of the catenary, r is the distance between the lines, and the magnet bore, ϕ, is the angle between the direction of the main field and that of the track, a current variation ΔI in the lines will induce the following field variation:

$$\Delta B_0 = \frac{2 \cdot \Delta I}{4\pi\varepsilon_0 c^2} \cdot \frac{h}{r^2} \cdot \cos\varphi. \qquad [7]$$

With $h = 5$ m, $r = 38$ m, $\phi = 24°$, $\Delta I = 4000$ A, and $\epsilon_0 =$ the permittivity of the void, the field variation B_0 is about 1.10^{-7} T. This value is similar to the measured field variation calculated from the MRI signal. Though the model is not refined (the train track is not linear and there may be shielding by metal objects), the measured and theoretical values are close. Thus, the amplitude and time scale of the variation indicate that our hypothesis that the power line caused B_0 to drift was reasonable.

Navigator echoes have been defined as additional non-phase encoded echoes that are acquired either before (6) or after (9) the main imaging echo trains. They have been used to correct involuntary (10,11) or physiological (2) motion. Our work shows that self-navigator echoes can also be used to monitor the fluctuations in the principal magnetic field, B_0, that can cause pseudo image-to-image motion. Other approaches have been proposed to correct for spatial field heterogeneities (12).

CONCLUSIONS

We have shown how an apparent displacement artifact along the phase-encoding direction was caused by a fluctuation of the principal magnetic field B_0. This fluctuation was due to variations in the current intensity of a nearby train power line. We used the central line as a self-navigator echo to simply and easily monitor changes in B_0 and thus correct the artifact. The amplitude and time scale of the observed variations were consistent with the data provided by the train company. Though such a correction would be irrelevant in the context of most MRI applications, in which motion under 1 mm remains negligible, it can be important in fMRI experiments, in which true or apparent displacement artifacts might cause false activation patterns. Hence, one should be aware of the possibility of such B_0 fluctuation related artifacts when using EPI sequences for fMRI studies.

ACKNOWLEDGMENTS

We thank Peter Jezzard for kindly providing some of the sources for acquisition and postprocessing. We also thank Mr. Leduc from the Régie Autonome des Transports Parisiens (RATP) for information on the power lines, and Patrick Leroux and Christian Leninte of General Electric Medical Systems, Buc, France, for their invaluable contributions.

REFERENCES

1. Foo TK, Hayes CE. Phase-correction method for reduction of B0 instability artifacts. J Magn Reson Imaging 1993;3:676–681.
2. Hu X, Kim SG. Reduction of signal fluctuation in functional MRI using navigator echoes. Magn Reson Med 1994;31:495–503.
3. Haacke M, Brown R, Thompson M, Venkatesan R. Magnetic resonance imaging—physical principles and sequence design. New York: Wiley-Liss; 1999. 914 p.
4. Jezzard P. Effects of B0 magnetic field drift on echo planar functional magnetic resonance imaging. In: Proceedings of the 4th Annual Meeting of ISMRM, 1996, New York. p 1817.
5. Glover GH, Lai S. Self-navigated spiral fMRI: interleaved versus single-shot. Magn Reson Med 1998;39:361–368.
6. Ehman RL, Felmlee JP. Adaptive technique for high-definition MR imaging of moving structures. Radiology 1989;173:255–263.
7. Jehenson P, Syrota A. Correction of distortions due to the pulsed magnetic field gradient-induced shift in B0 field by postprocessing. Magn Reson Med 1989;12:253–256.
8. Schmitt F, Stehling MK, Turner R. Echo-planar imaging: theory, technique and application. Berlin: Springer-Verlag; 1998. 662 p.
9. de Crespigny AJ, Marks MP, Enzmann DR, Moseley ME. Navigated diffusion imaging of normal and ischemic human brain. Magn Reson Med 1995;33:720–728.
10. Anderson AW, Gore JC. Analysis and correction of motion artifacts in diffusion weighted imaging. Magn Reson Med 1994;32:379–387.
11. Ordidge RJ, Helpern JA, Qing ZX, Knight RA, Nagesh V. Correction of motional artifacts in diffusion-weighted MR images using navigator echoes. Magn Reson Imaging 1994;12:455–460.
12. Irarrazabal P, Meyer CH, Nishimura DG, Macovski A. Inhomogeneity correction using an estimated linear field map. Magn Reson Med 1996;35:278–282.